

**Infrared absorption of the hydrogen donor in rutile TiO<sub>2</sub>**F. Herklotz, E. V. Lavrov,<sup>\*</sup> and J. Weber*Technische Universität Dresden, D-01062 Dresden, Germany*

(Received 4 April 2011; revised manuscript received 18 April 2011; published 1 June 2011)

Interstitial hydrogen in rutile TiO<sub>2</sub> is studied by infrared (IR) absorption. The measurements identify this defect as a shallow donor with an ionization energy of  $10 \pm 1$  meV. The IR absorption lines at around  $3290 \text{ cm}^{-1}$  include local vibrational modes (LVMs) of the neutral and the positive charge states of the donor. The neutral charge state reveals two LVMs at  $3288.3$  and  $3292.0 \text{ cm}^{-1}$ , whereas the positive charge state has a vibrational mode at  $3287.4 \text{ cm}^{-1}$ .

DOI: [10.1103/PhysRevB.83.235202](https://doi.org/10.1103/PhysRevB.83.235202)

PACS number(s): 78.30.Fs, 61.72.-y, 71.55.Gs

**I. INTRODUCTION**

TiO<sub>2</sub> in its two modifications, rutile and anatase, has been a subject of extensive studies since the discovery of the photocatalytic splitting of water at a TiO<sub>2</sub> electrode under ultraviolet (UV) light exposure in 1972.<sup>1,2</sup> The unique chemical, photochemical, and physical properties of this material in combination with the possibility of easy fabrication of nanostructures has led to numerous promising applications in areas ranging from photovoltaics and photocatalysis to photo-/electrochromics and sensors.<sup>3–6</sup> These exciting potential applications are in contrast to the poor understanding of fundamental processes like carrier excitation and transport in this material.

As-grown TiO<sub>2</sub> crystals of both types exhibit a rather high *n*-type carrier concentration. There is an ongoing dispute on the microscopic nature of the involved shallow donors. Mostly oxygen vacancies or titanium interstitials (Ti<sub>i</sub>) were discussed first as the source of *n*-type doping.<sup>7,8</sup> However, the electron paramagnetic resonance (EPR) identification of Ti<sub>i</sub> in rutile was reinterpreted and the observed center was ascribed to H impurities.<sup>9</sup> In support, shallow donor states for hydrogen were reported from conductivity<sup>10</sup> and transport measurements,<sup>11</sup> as well as from muon spin-rotation spectra in both rutile and anatase.<sup>12</sup> Ionization energies for the shallow donor are either not reported or vary drastically. Several calculations predict a shallow donor level for H in rutile.<sup>13–16</sup> However, a deep donor level is found if the interaction with the *d* electrons and polaronic effects are accounted for.<sup>17</sup> The behavior of hydrogen in TiO<sub>2</sub> appears to be far from trivial in other ways as well. A giant enhancement of diffusivity (important for storage purposes) was observed on electron irradiation<sup>18</sup> and infrared (IR) illumination.<sup>19</sup>

Early IR absorption experiments on rutile TiO<sub>2</sub> revealed a variety of hydrogen-related defects by their local vibrational modes.<sup>20,21</sup> Of particular interest for the present investigation is a defect that gives rise to a local vibrational mode (LVM) at  $3290 \text{ cm}^{-1}$  (10 K) originating from an O–H bond oriented perpendicular to the *c* axis of the crystal.<sup>20</sup> The defect responsible for this mode was attributed to an H<sup>+</sup>, which forms a single dative bond to oxygen using the O 2*p* lone-pair electrons. This behavior is in contrast with ZnO where hydrogen breaks an Zn–O bond to form an O–H complex. In rutile the hydrogen is located in the empty *c* channel and vibrates in a double-well potential between two O ions.<sup>19,22,23</sup>

We will label this defect H<sub>c</sub> or D<sub>c</sub> in the case of hydrogen or deuterium, respectively.

Here we assign the shallow hydrogen donor in rutile to the H<sub>c</sub> defect that gives rise to the  $3290 \text{ cm}^{-1}$  vibrational band. The ionization energy of the donor is in the order of meV. Our results provide insight into the microscopic and electrical properties of hydrogen and the electronic conductivity of rutile TiO<sub>2</sub>.

**II. EXPERIMENTAL**

The rutile TiO<sub>2</sub> samples used in this work were commercial (110)-oriented  $10 \times 10 \times 0.5 \text{ mm}^3$  wafers purchased from CrysTec GmbH (Germany). The nominally undoped single crystals were grown by the Verneuil technique and had a resistivity above  $10 \text{ M}\Omega \text{ cm}$  at room temperature (RT). Hydrogen and/or deuterium were/was introduced into the samples via thermal treatments in sealed quartz ampules filled with hydrogen and/or deuterium gas (pressure of 0.5 bar at RT). The treatments were carried out in the temperature range from  $480^\circ$  to  $530^\circ \text{C}$  for 12 to 18 h and were terminated by quenching to RT in water. In order to vary the concentration of hydrogen in the samples, isochronal treatments (anneals) in the temperature range  $500^\circ$  to  $630^\circ \text{C}$  were subsequently performed that had a duration of 30 min and were carried out in an argon atmosphere. The thermal stability of hydrogen donors was determined from a series of anneals at temperatures from  $100^\circ$  to  $900^\circ \text{C}$  in steps of  $50^\circ \text{C}$ .

Infrared absorption spectra were recorded with a Bomem DA3.01 Fourier transform spectrometer equipped with a global light source, a CaF<sub>2</sub> beamsplitter, and a liquid-nitrogen-cooled InSb detector. The spectral resolution was  $0.1\text{--}0.5 \text{ cm}^{-1}$ . Infrared absorption measurements were performed in a temperature range of  $5\text{--}110 \text{ K}$ . Polarized light was produced by a wire-grid polarizer with a KRS-5 substrate.

**III. RESULTS AND DISCUSSION**

A group of hydrogen-related local vibrational modes was detected at around  $3290 \text{ cm}^{-1}$  after annealing the TiO<sub>2</sub> samples in H<sub>2</sub> gas at  $525^\circ \text{C}$ . Figure 1 shows the evolution of the  $3290 \text{ cm}^{-1}$  feature at different sample temperatures. We note that no other hydrogen-related vibrational bands outside the region presented in the figure were observed. In accordance with previous studies (see Ref. 20), we found

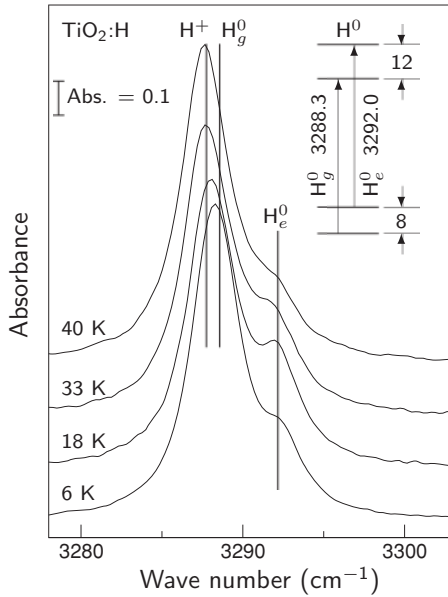


FIG. 1. Infrared absorption spectra (unpolarized light) of  $\text{TiO}_2\text{:H}$  recorded at different temperatures. The spectra are offset vertically for clarity. The inset shows energy level diagram (in  $\text{cm}^{-1}$ ) for the neutral charge state of  $\text{H}_c$ .

that these have a maximum intensity for the light polarized perpendicular to the  $c$  axis and anneal out at about  $550^\circ\text{C}$ . As-received  $\text{TiO}_2$  samples also reveal a weak (factor of 35 less) signal at  $3287.4\text{ cm}^{-1}$  with similar polarization properties. This mode, however, was found to be stable up to  $900^\circ\text{C}$  and we, therefore, conclude that the corresponding defect is related to an O–H bond close to another impurity or native defect.

$\text{TiO}_2$  samples treated in  $\text{D}_2$  reveal LVMs due to  $\text{D}_c$  at about  $2445\text{ cm}^{-1}$  with linewidths of about a factor of 2 smaller than those originating from  $\text{H}_c$ . Because of this, in the following discussion we will concentrate on the results obtained for the deuterium counterpart of this defect without, however, loss of generality.

Figure 2 shows IR absorption spectra recorded at 6, 17, 36, and 50 K for the  $\text{D}_c$  complex. Three lines at  $2445.0$ ,  $2445.7$ , and  $2447.8\text{ cm}^{-1}$  are clearly seen. Below we will give strong evidence that  $\text{D}_c$  is a shallow donor with the  $2445.0\text{ cm}^{-1}$  line originating from the positive charge state of this defect,  $\text{D}_c^+$ , whereas the  $2445.7$  and  $2447.8\text{ cm}^{-1}$  lines are due to the ground and an excited vibrational mode of the neutral state,  $\text{D}_c^0$ . We label these LVMs  $\text{D}^+$ ,  $\text{D}_g^0$ , and  $\text{D}_e^0$ , respectively. The corresponding modes of  $\text{H}_c$  are at  $3287.4$  ( $\text{H}^+$ ),  $3288.3$  ( $\text{H}_g^0$ ), and  $3292.0\text{ cm}^{-1}$  ( $\text{H}_e^0$ ).

First, we discuss the temperature behavior of  $\text{D}_g^0$  and  $\text{D}_e^0$ . As follows from Fig. 2, the  $\text{D}_g^0$  mode dominates the spectrum at 6 K. As the temperature raises, the intensity of the excited  $\text{D}_e^0$  mode grows in at the expense of  $\text{D}_g^0$ . Further increase in the temperature results in the broadening of both lines. The intensity ratio  $R$  of the  $\text{D}_e^0$  and  $\text{D}_g^0$  modes can be fit by the Boltzmann exponent  $R \propto \exp(-\Delta E_D/kT)$  with  $\Delta E_D \approx (1.2 \pm 0.1)\text{ meV} \approx (10 \pm 1)\text{ cm}^{-1}$ . Insert in Fig. 2 shows the energy level diagram of  $\text{D}_c^0$  deduced from the temperature-dependent measurements. In the case of hydrogen the ground state of  $\text{H}_c^0$  is split by  $\Delta E_H \approx$

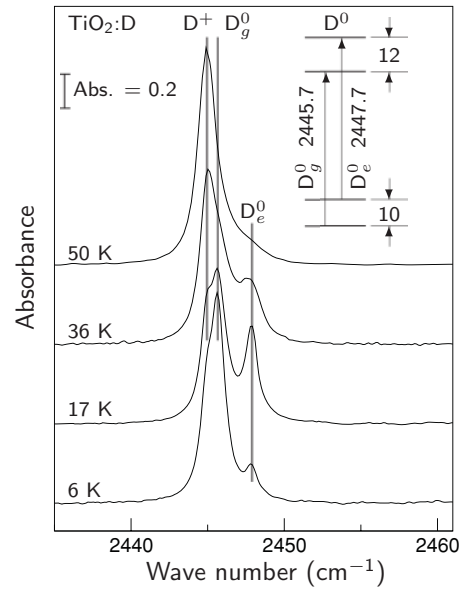


FIG. 2. Infrared absorption spectra (unpolarized light) of  $\text{TiO}_2\text{:D}$  recorded at different temperatures. The spectra are offset vertically for clarity. The inset shows the energy level diagram (in  $\text{cm}^{-1}$ ) for the neutral charge state of  $\text{D}_c$ .

$(1.00 \pm 0.05)\text{ meV} \approx (8 \pm 0.5)\text{ cm}^{-1}$ . The energy-level diagram is given as an inserts in Fig. 1.

At present we can only speculate about the origin of the LVM splitting of  $\text{H}_c^0$  ( $\text{D}_c^0$ ). Polaron effects due to the localized donor electron at a Ti ion seem to be possible as well as electronic splitting of the ground donor state. Another plausible explanation of the splitting comes from the microscopic structure of the defect. According to theory, the proton (deuteron) is located inside the  $c$  channel of the rutile lattice in a double-well potential along the O–O direction perpendicular to the  $c$  axis.<sup>22</sup> Due to the asymmetry of the potential, the proton (deuteron) is localized in one minimum.<sup>24</sup> The finite energy barrier between the two minima, however, leads to a tunneling splitting of the vibrational states of the proton (deuteron). Note that a similar behavior was recently observed for hydrogen in  $\text{KTaO}_3$ .<sup>25</sup> The tunneling splitting is larger for smaller barrier heights, which qualitatively explains the “blue” shift of the excited vibrational level compared to the ground one (see insets in Figs. 1 and 2). The significant broadening of the LVMs for  $T > 25\text{ K}$  may then be due to the incoherent tunneling caused by the lattice vibration and the associated modulation of the proton potential.<sup>24,25</sup> However, with regard to this explanation the difference in the ground-state splitting between the hydrogen isotopes is relatively small. Further experimental as well as theoretical studies are needed to clarify this issue.

Dependence of LVM frequencies of hydrogen-related defects on the charge state has been documented in many semiconductors, e.g., GaAs,<sup>26</sup> Si,<sup>27</sup> or ZnO.<sup>28</sup> Typically, these defects give rise to deep rather than shallow levels in the band gap. Below we present the evidences that the  $\text{H}^+$  ( $\text{D}^+$ ) mode and the  $\text{H}^0$  ( $\text{D}^0$ ) modes of  $\text{H}_c$  ( $\text{D}_c$ ) are due to the positive and neutral charge state of a shallow donor, respectively.

Figure 3(a) shows the integrated absorption measured on the  $\text{D}^+$  and  $\text{D}^0$  modes as a function of temperature. The two

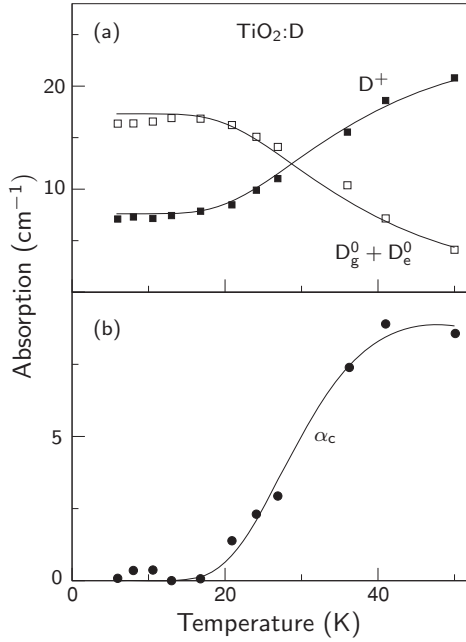


FIG. 3. Absorption of  $D^+$  (■),  $D_g^0+D_e^0$  (□) (a), and free carriers  $\alpha_c$  (●) (b) as a function of temperature obtained from a  $TiO_2$  sample treated in the  $D_2$  gas. The solid lines are the best-fit curves of the experimental data (see text).

signals are constant for the temperatures below 20 K. As the temperature raises, the intensity of  $D^+$  grows in, whereas that of  $D^0$  weakens. The anticorrelation between vibrational modes of  $D^+$  and  $D^0$  confirms our suggestion that they originate from different charge states of the same defect. The temperature dependence shown in the figure can be fitted assuming that  $D_c$  is the dominant donor in the sample with some background acceptors. The latter follows from the nonvanishing intensity of the  $D^+$  mode at low temperatures. In this model the concentration of the ionized donors  $N^+$  is obtained from (see e.g., Ref. 29)

$$\frac{N^+}{N_D} = \frac{N_A - x}{2N_D} + \sqrt{\left(\frac{N_A - x}{2N_D}\right)^2 + \frac{x}{N_D}}. \quad (1)$$

Here,  $N_A$  is the concentration of the compensating acceptors,  $E_D$  the ionization energy of the shallow donor,  $m_e^*$  the electron effective mass,  $x = 0.5N_c \exp(-E_D/k_B T)$ , and  $N_c = 2(m_e^* k_B T / 2\pi \hbar^2)^{3/2}$ . A reasonably good agreement with the experimental data shown in Fig. 3(a) by the solid lines is obtained for  $E_D = (10 \pm 1)$  meV,  $N_D = (2.5 \pm 0.5) \times 10^{16} \text{ cm}^{-3}$ ,  $N_A = (8 \pm 3) \times 10^{15} \text{ cm}^{-3}$ , and  $m_e^* = (17.0 \pm 1.5)m_e$ . Note that due to the anisotropy of the conduction band of rutile  $m_e^* = (m_{\parallel} m_{\perp}^2)^{1/3}$ , where  $m_{\parallel}$  and  $m_{\perp}$  are the effective mass parameters of the ellipsoidal energy minimum with the main axes parallel and perpendicular to the  $c$  axis, respectively.<sup>30</sup>

Within the experimental accuracy, the results obtained for the same  $TiO_2$  material treated in the  $H_2$  gas yielded the same values of  $E_D$ ,  $m_e^*$ , and  $N_A$ . The independence of these parameters on the hydrogen isotope supports the shallow donor nature of  $H_c$ . Moreover, the results of this fit allow us to calibrate the integrated intensity of the LVMs at

$3290 \text{ cm}^{-1}$  in order to determine the total concentration  $N$  of these defects,

$$N = 6.6 \times 10^{14} \text{ cm}^{-1} \int \alpha_{3290}(\sigma) d\sigma. \quad (2)$$

Here,  $\sigma$  is the wave number. The absorption coefficient is inversely proportional to the reduced mass  $m_r$  of vibrating species.<sup>31</sup> We found that in the case of LVMs of  $D_c$ , the corresponding prefactor in Eq. (2) equals  $1.2 \times 10^{15} \text{ cm}^{-1}$ . This is approximately a factor of 2 higher compared to hydrogen, which is in good agreement with the ratio  $m_r^D/m_r^H = 1.9$ , where  $m_r^H$  and  $m_r^D$  are the reduced masses of the  $^{16}\text{O}-\text{H}$  and  $^{16}\text{O}-\text{D}$  units, respectively.

The effective mass of electrons in the conduction band of rutile was determined previously by the Hall effect and conductivity,<sup>11,32,33</sup> IR reflectivity,<sup>34</sup> optical absorption,<sup>35</sup> thermoelectric effect,<sup>33,36,37</sup> and specific heat measurements.<sup>38</sup> The reported values, however, are spread in a wide range between  $2 m_e$  and  $190 m_e$ . We speculate that such a discrepancy originates from variations of intrinsic defects in the different samples. Note that most of the studies cited above were performed at RT. On the other hand, the values of  $m_e^*$  deduced from the low-temperature measurements are  $12.5 m_e$  (6–40 K)<sup>11</sup> and  $8 m_e$  (1.6–300 K),<sup>35</sup> which is in reasonable agreement with the results of our measurements performed in the temperature range 6 to 110 K.

The ionization temperature of shallow defects  $T_a$ , which is defined as a temperature at which concentrations of neutral and ionized species are equal, depends on the total amount of the defects. In the case presented in Fig. 3(a) we see that  $T_a \approx 30$  K. In order to further test the shallow donor nature of  $H_c$  ( $D_c$ ), experiments similar to the one presented in Fig. 3 were carried out for different integrated intensities of the 3290 ( $2445$ )  $\text{cm}^{-1}$  modes (see experimental section for details). It was established that the value of  $T_a$  decreases as the integrated LVMs intensities due to  $H_c$  ( $D_c$ ) drop. Moreover, because of the compensating acceptors, which were always present in our samples, only the  $H^+$  ( $D^+$ ) modes were seen in the spectra for low concentrations of the species. These findings are also in favor of  $H_c$  ( $D_c$ ) as a shallow donor in  $TiO_2$ .

Free electrons in the conduction band of  $TiO_2$  also absorb light. Treated classically, the corresponding absorption coefficient  $\alpha_c$  is given by (see e.g., Ref. 39)

$$\alpha_c = \frac{4\pi e^2 n}{n_r c m_e^*} \frac{\tau}{1 + \omega^2 \tau^2}, \quad (3)$$

where  $n$  is the concentration of the electrons in the conduction band,  $n_r$  is the refractive index, and  $c$  is the speed of light. From the Drude model of electrical conduction, the mean relaxation time may be expressed as  $\tau = \mu m_e^*/e$ , where  $\mu$  is the electron drift mobility.

At temperatures below 10 K all carriers freeze-out so  $n$  is equal to zero. Therefore, the absorption spectrum taken at 5 K can be used as a reference signal to obtain the absorption coefficient due to free electrons  $\alpha_c = \alpha(T) - \alpha(5 \text{ K})$ . Figure 3(b) shows the value of  $\alpha_c$  determined at  $2400 \text{ cm}^{-1}$  in the temperature range 5 to 50 K for the same sample as in Fig. 3(a). As one can see, the free carrier absorption correlates quite well with the intensity of the  $D^+$  signal.

At low temperatures electrons are preferentially scattered at ionized centers.<sup>29,32,40</sup> The solid line in Fig. 3(b) is a fit of  $\alpha_c$  obtained under the assumption that this is the dominant scattering mechanism for temperatures below 50 K. A detailed discussion of the electron mobility in TiO<sub>2</sub> is beyond the scope of this paper. We refer to the Hall effect and conductivity studies of rutile TiO<sub>2</sub>.<sup>32,36,37,40–42</sup> Note that  $\mu$  was the only fitting parameter for the solid line in Fig. 3(b), since the values of  $m_c^*$  and  $n$  were obtained from the data presented in Fig. 3(a). At about 40 K the mobility has a maximum value of about 50 cm<sup>2</sup>/Vs. The reasonable agreement with the results of previous measurements is consistent with the model of D<sub>c</sub> (H<sub>c</sub>) as a shallow donor in rutile TiO<sub>2</sub>.

As a part of this investigation we also performed photoconductivity measurements for hydrogenated TiO<sub>2</sub>. It was established that the photosignal can be detected only at low temperatures when free electrons freeze-out. The freeze-out temperatures were found to correlate with the values of  $T_a$ , which we take as an additional support of the shallow donor nature of H<sub>c</sub>. A detailed photoconductivity investigation of TiO<sub>2</sub> will be performed separately.

Finally we want to comment on the thermal stability of H<sub>c</sub>. The activation energies of hydrogen diffusion in rutile TiO<sub>2</sub> parallel and perpendicular to the  $c$  axis were found to be 0.59 and 1.28 eV, respectively.<sup>43,44</sup> This makes isolated hydrogen extremely mobile already at room temperature and may, in principle, result in formation of interstitial H<sub>2</sub> molecules as it happens in ZnO.<sup>45</sup>

We performed Raman scattering measurements in the course of annealing process of H<sub>c</sub> to probe hydrogen molecules in TiO<sub>2</sub>. No signal was found, which would appear in the

spectra at the expense of the 3290 cm<sup>-1</sup> vibrational band. This is consistent with the results of first principles calculations which predict that H<sub>2</sub> is 2.4 eV higher in energy than two isolated H<sub>c</sub>.<sup>17</sup>

Recently, Chen *et al.* reported the results of the I-V measurements of electrochemically hydrogenated TiO<sub>2</sub>.<sup>46</sup> These authors established that the I-V characteristics of rutile hydrogenated at RT reveal a strong aging behavior. This finding was interpreted in terms of H<sup>+</sup> diffusion with subsequent formation of electrically inactive H<sub>2</sub>. The mobile H<sup>+</sup> species was assigned to some unknown metastable state of hydrogen which does not form an O–H bond.

In our opinion, H<sub>c</sub><sup>+</sup> alone can account for the aging behavior of TiO<sub>2</sub> reported by Chen *et al.* The low activation energy of H<sub>c</sub> diffusion<sup>19,43,44</sup> together with the high formation energy of H<sub>2</sub> implies that the apparent thermal stability of hydrogen donors in rutile detected by these authors depends on the experimental conditions such as presence of traps, sample thickness, concentration profile, and so on.

#### IV. SUMMARY

The hydrogen-related defect in rutile TiO<sub>2</sub> that gives rise to the vibrational modes at around 3290 cm<sup>-1</sup> was identified as a shallow donor with an ionization energy of 10 ± 1 meV. The 3290 cm<sup>-1</sup> feature consists of two LVMS due to the neutral and the positive charge states of the donor with relative intensities depending on the sample temperature. In the neutral charge state, the defect reveals two LVMS at 3288.3 and 3292.0 cm<sup>-1</sup>. The positive charge state results in a vibrational mode at 3287.4 cm<sup>-1</sup>.

\*edward.lavrov@physik.tu-dresden.de

<sup>1</sup>A. Fujishima and K. Honda, *Nature* **238**, 37 (1972).

<sup>2</sup>A. Fujishima, T. N. Rao, and D. A. Tryk, *Electrochim. Acta* **45**, 4683 (2000).

<sup>3</sup>M. Grätzel, *Nature* **414**, 338 (2001).

<sup>4</sup>A. Hagfeldt and M. Graetzel, *Chem. Rev.* **95**, 49 (1995).

<sup>5</sup>A. L. Linsebigler, G. Lu, and J. T. Yates, *Chem. Rev.* **95**, 735 (1995).

<sup>6</sup>A. Millis and S. L. Hunte, *J. Photochem. Photobiol.* **108**, 1 (1997).

<sup>7</sup>M. K. Nowotny, T. Bak, and J. Nowotny, *Phys. Chem. B* **110**, 16283 (2006).

<sup>8</sup>K. H. Kim, E. J. Oh, and J. S. Choi, *J. Phys. Chem. Solids* **45**, 1265 (1984).

<sup>9</sup>L. N. Shen, O. W. Johnson, W. D. Ohlsen, and J. W. DeFord, *Phys. Rev. B* **10**, 1823 (1974).

<sup>10</sup>P. F. Chester and D. H. Bradhurst, *Nature* **199**, 1056 (1963).

<sup>11</sup>J. W. DeFord and O. W. Johnson, *J. Appl. Phys.* **54**, 889 (1983).

<sup>12</sup>S. F. J. Cox, J. S. Lord, S. P. Cottrell, J. M. Gil, H. V. Alberto, A. Keren, D. Prabhakaran, R. Scheuermann, and A. Stoykov, *J. Phys. Condens. Mat.* **18**, 1061 (2006).

<sup>13</sup>C. Kilic and A. Zunger, *Appl. Phys. Lett.* **81**, 73 (2002).

<sup>14</sup>P. W. Peacock and J. Robertson, *Appl. Phys. Lett.* **83**, 2025 (2003).

<sup>15</sup>J. Robertson and P. W. Peacock, *Thin Solid Films* **445**, 155 (2003).

<sup>16</sup>K. Xiong, J. Robertson, and S. J. Clark, *J. Appl. Phys.* **102**, 083710 (2007).

<sup>17</sup>F. Filippone, G. Mattioli, P. Alippi, and A. Amore Bonapasta, *Phys. Rev. B* **80**, 245203 (2009).

<sup>18</sup>Y. Chen, R. Gonzalez, and K. L. Tsang, *Phys. Rev. Lett.* **53**, 1077 (1984).

<sup>19</sup>E. J. Spahr, L. Wen, M. Stavola, L. A. Boatner, L. C. Feldman, N. H. Tolk, and G. Lüpke, *Phys. Rev. Lett.* **104**, 205901 (2010).

<sup>20</sup>B. H. Soffer, *J. Chem. Phys.* **35**, 940 (1961).

<sup>21</sup>O. W. Johnson, W. D. Ohlsen, and P. L. Kingsbury, *Phys. Rev.* **175**, 1102 (1968).

<sup>22</sup>M. V. Koudriachova, S. W. de Leeuw, and N. M. Harrison, *Phys. Rev. B* **70**, 165421 (2004).

<sup>23</sup>R. J. Swope, J. R. Smyth, and A. C. Larson, *Am. Mineral.* **80**, 448 (1995).

<sup>24</sup>P. G. Johannsen, *J. Phys. Condens. Matter* **10**, 2241 (1998).

<sup>25</sup>E. J. Spahr, L. Wen, M. Stavola, L. A. Boatner, L. C. Feldman, N. H. Tolk, and G. Lüpke, *Phys. Rev. Lett.* **102**, 075506 (2009).

<sup>26</sup>B. Clerjaud, D. Côte, W.-S. Hahn, A. Lebkiri, W. Ulrici, and D. Wasik, *Phys. Status Solidi A* **159**, 121 (1987).

<sup>27</sup>V. A. Gordeev, R. F. Konopleva, V. G. Firsov, Yu. V. Obukhov, Yu. V. Gorelinskii, and N. N. Nevinnyi, *Hyp. Int.* **60**, 717 (1990).

<sup>28</sup>F. Herklotz, E. V. Lavrov, V. I. Kolkovskiy, J. Weber, and M. Stavola, *Phys. Rev. B* **82**, 115206 (2010).

<sup>29</sup>K. Seeger, *Semiconductor Physics*, 9th ed. (Springer, Berlin, 2004).

<sup>30</sup>T. H. Geballe, in *Semiconductors*, edited by N. B. Hannay (Reinhold, New York, 1959).

- <sup>31</sup>E. B. Wilson, J. C. Decius, and P. C. Cross, *Molecular Vibrations* (Dover, New York, 1980).
- <sup>32</sup>E. Yagi, R. R. Hasiguti, and M. Aono, *Phys. Rev. B* **54**, 7945 (1996).
- <sup>33</sup>M. Itakura, N. Nizeki, H. Toyoda, and H. Iwasaki, *Jpn. J. Appl. Phys.* **6**, 311 (1967).
- <sup>34</sup>J.-F. Baumard and F. Gervais, *Phys. Rev. B* **15**, 2316 (1977).
- <sup>35</sup>J. Pascual, J. Camassel, and H. Mathieu, *Phys. Rev. B* **18**, 5606 (1978).
- <sup>36</sup>H. P. R. Frederikse, *J. Appl. Phys.* **32**, 2211 (1961).
- <sup>37</sup>G. A. Acket and J. Volger, *Physica* **32**, 1680 (1966).
- <sup>38</sup>T. R. Sandin and P. H. Keesom, *Phys. Rev.* **177**, 1370 (1969).
- <sup>39</sup>P. Y. Yu and M. Cardona, *Fundamentals of Semiconductors: Physics and Materials Properties*, 4th ed. (Springer, Berlin, 2010).
- <sup>40</sup>F. A. Grant, *Rev. Mod. Phys.* **31**, 646 (1959).
- <sup>41</sup>V. N. Bogomolov and V. P. Zhuze, *Sov. Phys. Solid State* **8**, 1904 (1967).
- <sup>42</sup>R. Ramaneti, J. C. Lodder, and R. Jansen, *Phys. Rev. B* **76**, 195207 (2007).
- <sup>43</sup>O. W. Johnson, S.-H. Paek, and J. W. DeFord, *J. Appl. Phys.* **46**, 1026 (1975).
- <sup>44</sup>J. B. Bates, J. C. Wang, and R. A. Perkins, *Phys. Rev. B* **19**, 4130 (1979).
- <sup>45</sup>E. V. Lavrov, F. Herklotz, and J. Weber, *Phys. Rev. Lett.* **102**, 185502 (2009).
- <sup>46</sup>W. P. Chen, Y. Wang, and H. L. W. Chan, *Appl. Phys. Lett.* **92**, 112907 (2008).